



# Ab initio thermal expansion and thermoelastic properties of ringwoodite ( $\gamma$ -Mg<sub>2</sub>SiO<sub>4</sub>) at mantle transition zone conditions

Donato Belmonte<sup>1,2</sup>, Mattia La Fortezza<sup>1</sup>, and Francesca Menescardi<sup>1</sup>

<sup>1</sup>DISTAV, University of Genoa, Genoa, 16132, Italy

<sup>2</sup>Italian National Antarctic Museum (MNA, Section of Genoa), University of Genoa, Genoa, 16132, Italy

**Correspondence:** Donato Belmonte (donato.belmonte@unige.it)

Received: 6 October 2021 – Revised: 18 February 2022 – Accepted: 25 February 2022 – Published: 24 March 2022

**Abstract.** Thermal convection in the Earth's mantle is driven by lateral variations in temperature and density, which are substantially controlled by the local volume thermal expansion of the constituent mineral phases. Ringwoodite is a major component of the lower mantle transition zone, but its thermal expansivity and thermoelastic properties are still affected by large uncertainties. Ambient thermal expansion coefficient ( $\alpha_{V_0}$ ), for instance, can vary as much as 100 % according to different experimental investigations available from the literature. In this work, we perform ab initio density functional theory calculations of vibrational properties of spinel-structured Mg<sub>2</sub>SiO<sub>4</sub> ringwoodite in order to provide reliable thermophysical data up to mantle transition zone conditions. Temperature- and pressure-dependent thermal expansivity has been obtained by phonon dispersion calculations in the framework of quasi-harmonic approximation (QHA) up to 25 GPa and 2000 K. Theoretical analysis of vibrational spectra reveals that accurate prediction of IR and silent modes, along with their relative mode Grüneisen parameters, is crucial to define thermal expansivity. A six-parameter analytical function is able to reproduce ab initio values fairly well in the whole investigated  $P$ - $T$  range, i.e.,  $\alpha_V(P, T) = (1.6033 \times 10^{-5} + 8.839 \times 10^{-9}T + 11.586 \times 10^{-3}T^{-1} - 6.055T^{-2} + 804.31T^{-3}) \times \exp(-2.52 \times 10^{-2}P)$ , with temperature in kelvin and pressure in gigapascal. Ab initio static and isothermal bulk moduli have been derived for ringwoodite along with their  $P$ ,  $T$  and cross derivatives, i.e.,  $K_0 = 184.3$  GPa,  $K_{T,300\text{K}} = 176.6$  GPa,  $K'_0 = 4.13$ ,  $K'_{T,300\text{K}} = 4.16$ ,  $\left(\frac{\partial K_T}{\partial T}\right)_P = -0.0233$  GPa K<sup>-1</sup> and  $\left(\frac{\partial^2 K_T}{\partial P \partial T}\right)_0 = 1.0 \times 10^{-4}$  K<sup>-1</sup>. Computed thermal expansivity and thermoelastic properties support the evidence that QHA performs remarkably well for Mg<sub>2</sub>SiO<sub>4</sub> ringwoodite up to mantle transition zone temperatures. Since volume thermal expansion of ringwoodite is strongly pressure-dependent and its pressure dependence becomes more marked with the increasing temperature, internally consistent assessments and empirical extrapolation of thermoelastic data to deep mantle conditions should be taken with care to avoid inaccurate or spurious predictions in phase equilibrium and mantle convection numerical modeling.

## 1 Introduction

Despite the development of internally consistent databases for planetary materials, thermodynamic properties of deep mantle minerals are still poorly constrained or even completely lacking at high pressure and temperature conditions (HP-HT). Relevant geophysical properties like volume thermal expansion and isothermal bulk modulus can be derived

from experimental measurements at ambient pressure in the low- to medium-temperature range, but they are usually less defined at higher temperatures (and pressures) due to technical problems or conditions of the samples, especially when melting or decomposition may occur (Thieblot et al., 1998; Fiquet et al., 1999). For these reasons large extrapolation of thermophysical data is often invoked at HP-HT without any warranty of physical soundness (Helffrich, 1999). Inaccu-

rate thermodynamic properties could in turn strongly affect the prediction of phase equilibrium and stability relations of mantle minerals at deep Earth conditions.

Ringwoodite is a major constituent phase of the lowermost mantle transition zone (MTZ), between  $\sim 520$  and  $660$  km depths, where its relative amount is estimated to be between  $\sim 40\%$  vol and  $60\%$  vol according to different compositional models of the Earth's mantle (Ringwood, 1975; Bass and Anderson, 1984). It is now generally accepted that spinel and post-spinel phase transformations of olivine play a key role in determining global mantle discontinuities in the middle and bottom part of the transition zone (Bina and Helffrich, 1994; Sinogeikin et al., 2003; Ishii et al., 2019), although the ultimate origin, sharpness and seismic signature of the  $520$  and  $660$  km discontinuities are still a matter of debate (e.g., Deuss and Woodhouse, 2001; Deuss et al., 2006; Saikia et al., 2008). This basically reflects the still unconstrained abundance of olivine versus non-olivine mineral phases (majoritic garnet above all) in this part of the mantle and the fact that their stability field, density and thermoelastic properties are roughly compatible with seismic impedance contrasts and velocity jumps observed by global seismology (Shearer, 1996; Deuss et al., 2006; Schmerr and Garnero, 2007). In any case, the thermodynamic behavior of ringwoodite has a significant impact on physicochemical processes of the mantle transition zone (Akaogi et al., 2007; Kojitani et al., 2016). The natural occurrence of ringwoodite with normal spinel structure in many shocked chondritic meteorites (e.g., Chen et al., 2004) and as a mineralogical inclusion in ultradeep diamonds from Juína, Brazil (Pearson et al., 2014), further supports this evidence. Structural inversion may have a potential effect (Kiefer et al., 1999; Panero, 2008; Bindi et al., 2018), but thermodynamic considerations suggest that Mg-endmember ringwoodite is unlikely to be stable in the inverse spinel phase in the Earth's transition zone.

In this work we perform ab initio density functional theory calculations of vibrational properties and volume thermal expansion of spinel-structured  $\text{Mg}_2\text{SiO}_4$  ringwoodite in the framework of quasi-harmonic approximation (QHA) in order to provide reliable thermophysical data up to mantle transition zone conditions. This study is part of a broader project aimed at setting up a comprehensive high-pressure thermodynamic database for solid-state and solid-liquid phase equilibrium calculations in geochemically relevant multi-component systems by “ab initio assisted” computational thermodynamics (Belmonte et al., 2017a, b). A detailed survey of the available experimental and theoretical data on Raman and IR spectra, isothermal bulk modulus, volume thermal expansion, and thermal expansivity of  $\text{Mg}_2\text{SiO}_4$  ringwoodite is carried out to show how relevant current uncertainties on the physicochemical behavior of this important building block of planetary interiors might be. By giving a theoretical constraint to the extrapolation of thermodynamic data at MTZ depths, ab initio calculations performed in this work allow us to infer some relevant insights into the role of

ringwoodite in mantle dynamics, as briefly discussed in the implications section.

## 2 Computational method

Ab initio calculations in this work have been performed by using the LCAO (linear combination of atomic orbitals) approach with an all-electron Gaussian-type basis set as implemented in the CRYSTAL code (Dovesi et al., 2014). The hybrid B3LYP density functional, which contains  $20\%$  of exact Hartree–Fock exchange mixed with generalized gradient approximation (GGA) exchange–correlation (Becke, 1993; Lee et al., 1988), has been employed due to its high performance on vibrational, elastic and thermodynamic properties of a large variety of insulating crystalline phases (e.g., Otonello et al., 2010; Belmonte et al., 2013; Erba et al., 2014; Belmonte et al., 2016). The basis set for Mg, Si and O atoms and computational parameters are the same as those used in our previous investigations on dense magnesium silicates and oxides and can be found elsewhere (see De La Pierre and Belmonte, 2016 and Belmonte, 2017, for full details).

Phonon dispersion calculations at  $\mathbf{q}$  points other than  $\Gamma$  have been performed on large isotropic or anisotropic supercells with the direct method (see Parlinski et al., 1997; Evarestov and Losev, 2009). In order to check numerical convergence on calculated thermal expansion and thermoelastic properties, a total of  $18$   $\mathbf{q}$  points in the first Brillouin zone have been sampled by using  $2 \times 2 \times 2$ ,  $3 \times 1 \times 1$ ,  $1 \times 3 \times 1$ ,  $1 \times 1 \times 3$ ,  $3 \times 2 \times 1$  and  $3 \times 1 \times 2$  supercells and exploiting the cubic symmetry of the ringwoodite structure (space group  $Fd\bar{3}m$ ). Once phonon modes have been computed on the fully relaxed equilibrium structure, their volume dependence has been defined in the framework of quasi-harmonic approximation (QHA) (e.g., Wallace, 1972). Mode Grüneisen parameters of phonon modes ( $\gamma_i$ ) are thus obtained as follows:

$$\gamma_i(\mathbf{q}, V) = -\frac{\partial \ln \nu_i(\mathbf{q}, V)}{\partial \ln V}, \quad (1)$$

where  $\nu_i$  is the wavenumber of the  $i$ th vibrational mode of the crystal lattice sampled at discrete  $\mathbf{q}$  points in the first Brillouin zone, and  $V$  is the volume of the unit cell. Thus, also the effect of phonon dispersion on mode Grüneisen parameters has been defined by the supercell approach in this work. Least-square fitting of vibrational frequencies computed at five different volume conditions (i.e.,  $V/V_0 \cong 0.89, 0.92, 0.96, 0.98$  and  $1.00$ ) gives the values of  $\gamma_i$  for all modes. Linear or second-order polynomial fitting accurately describes the volume dependence of all the vibrational frequencies in the investigated compression range. The calculated equation of state (EOS) for  $\text{Mg}_2\text{SiO}_4$  ringwoodite allows us to convert volume dependence of vibrational frequencies into pressure dependence for a direct comparison with experimental measurements (see Sect. 3).

### 3 Results and discussion

#### 3.1 Vibrational properties at ambient and high-pressure conditions

The experimental characterization of the full vibrational spectra of deep mantle minerals at ambient and non-ambient conditions is still challenging. One of the reasons for the overwhelming success of theoretical investigations based on density functional theory (DFT) combined with the quasi-harmonic approximation (QHA) is that the full vibrational density of state (vDOS) of crystalline solids can be directly provided by phonon dispersion calculations. Physically consistent thermodynamic and thermoelastic properties can then be predicted for a broad range of  $P$ – $T$  conditions by statistical mechanics (Wallace, 1972).

Even though there are several IR and Raman spectroscopic studies on ringwoodite, most of them have been performed to characterize natural samples of shocked meteorites (e.g., Guyot et al., 1986; Chen et al., 2004; Feng et al., 2011; Acosta-Maeda et al., 2013) or mineral inclusions in diamonds (Pearson et al., 2014), while only a few experimental investigations focused on the Mg end-member (Akaogi et al., 1984; McMillan and Akaogi, 1987; Chopelas et al., 1994).

The zone-center optic vibrational modes of ringwoodite with cubic spinel structure (space group  $Fd\bar{3}m$ , point group  $m\bar{3}m$ ) can be classified by symmetry analysis as follows:

$$\Gamma_{\text{optic}} = A_{1g} \oplus 2A_{2u} \oplus E_g \oplus 2E_u \oplus T_{1g} \oplus 4T_{1u} \oplus 3T_{2g} \oplus 2T_{2u}, \quad (2)$$

where  $A_{1g}$ ,  $E_g$  and  $T_{2g}$  modes (symmetric with respect to inversion) are Raman active;  $T_{1u}$  modes (anti-symmetric with respect to inversion) are IR active; and  $A_{2u}$ ,  $E_u$ ,  $T_{1g}$  and  $T_{2u}$  modes are silent. Due to the high symmetry of the structure,  $E_g$  and  $E_u$  modes are doubly degenerate, while  $T_{1g}$ ,  $T_{1u}$ ,  $T_{2g}$  and  $T_{2u}$  modes are triply degenerate in the irreducible representations of Eq. (2). Vibrational frequencies as computed in this work by ab initio B3LYP calculations are compared to experimental results and other DFT calculations (Piekarz et al., 2002; Yu and Wentzcovitch, 2006; Li et al., 2009; Hernández et al., 2015) in Table S1 (see Supplement). Only transverse optic (TO) modes have been computed, as LO–TO splitting is relevant just for the IR-active  $T_{1u}$  modes (Piekarz et al., 2002), and its effect on thermodynamic properties as determined by phonon dispersion calculations is negligible.

The experimental Raman spectrum of  $\text{Mg}_2\text{SiO}_4$  ringwoodite shows two strong bands at 794–796 and 834–836  $\text{cm}^{-1}$  (assigned to  $T_{2g}$  and  $A_{1g}$  modes and corresponding to asymmetric and symmetric stretching of  $\text{SiO}_4^{4-}$  tetrahedra, respectively), along with weaker peaks at 302, 370–372 and 600  $\text{cm}^{-1}$  (McMillan and Akaogi, 1987; Chopelas et al., 1994). Ab initio B3LYP calculations predict the position of the two most intense Raman peaks within 3–5  $\text{cm}^{-1}$  and with the correct symmetry analysis. It is interesting to note that mode assignment in experimental studies could be rather

difficult. McMillan and Akaogi (1987) assigned the Raman band at 794  $\text{cm}^{-1}$  to the symmetric stretching vibration of Si–O tetrahedra with  $A_{1g}$  symmetry in their unpolarized powder spectrum, while Chopelas et al. (1994) correctly assigned it to asymmetric stretching with  $T_{2g}$  symmetry based on single-crystal oriented spectra. This mode assignment is confirmed also by other DFT studies (Piekarz et al., 2002; Yu and Wentzcovitch, 2006; Li et al., 2009; Hernández et al., 2015). The weaker Raman peaks are also accurately predicted, with a partial disagreement ( $\sim 20 \text{ cm}^{-1}$ ) for the  $T_{2g}$  mode at 619  $\text{cm}^{-1}$  (see Table S1 in the Supplement). By comparing experimental and theoretical investigations, the position of this peak is the most uncertain in the Raman spectrum, located in the region between  $\sim 570$  and 620  $\text{cm}^{-1}$ .

Four infrared bands are expected to be present in the IR spectrum of cubic silicate spinels (White and DeAngelis, 1967; Preudhomme and Tarte, 1971), although additional features could be present possibly due to some deviation from the cubic symmetry, structural disorder or vibrational coupling between octahedral and tetrahedral lattice modes (Jeanloz, 1980). Akaogi et al. (1984) observed only two major bands centered near 830 and 445  $\text{cm}^{-1}$  for  $\text{Mg}_2\text{SiO}_4$  ringwoodite, along with minor features corresponding to weak bands or shoulders at 920, 785, 510, 395 and 350  $\text{cm}^{-1}$ . The broadness of the major infrared bands found in experiments makes a direct comparison with our ab initio calculations, which correctly predict four IR-active  $T_{1u}$  modes with wavenumbers 341, 396, 545 and 802  $\text{cm}^{-1}$  (Table S1) difficult. B3LYP results are quite different from those obtained by other GGA calculations (Piekarz et al., 2002; Hernández et al., 2015), except for the predicted IR modes in the low-frequency range, which may differ by less than 10  $\text{cm}^{-1}$ . The same consideration roughly applies to computed frequencies for the silent modes.

In order to test the performance of ab initio B3LYP calculations, theoretical and experimental frequencies are compared by means of a global statistical index, which is defined as follows (see De La Pierre and Belmonte, 2016):

$$|\bar{\Delta}| = M^{-1} \sum_{i=1}^M |v_i^{\text{calc}} - v_i^{\text{exp}}|, \quad (3)$$

where  $M$  is the number of data considered in the statistics and  $|\bar{\Delta}|$  is the mean absolute difference between calculated ( $v_i^{\text{calc}}$ ) and experimentally observed frequencies ( $v_i^{\text{exp}}$ ). Only the frequencies of the five Raman-active modes (i.e.,  $A_{1g}$ , doubly degenerate  $E_g$  and triply degenerate  $T_{2g}$  modes) have been included in the statistics, since two different experimental studies give nearly coincident results (McMillan and Akaogi, 1987; Chopelas et al., 1994), and a direct comparison between ab initio and experimental data is not straightforward for the IR-active modes. In that case,  $M = 12$  and  $|\bar{\Delta}| = 7 \text{ cm}^{-1}$  if frequencies computed in this work at the B3LYP level of theory are compared with either the experimental dataset by McMillan and Akaogi (1987) or that by

Chopelas et al. (1994) (Table S1). The agreement with observed Raman spectra is thus excellent and markedly better than ab initio local density approximation (LDA) or GGA results, which give  $|\bar{\Delta}| = 10\text{--}12\text{ cm}^{-1}$  and  $|\bar{\Delta}| = 24\text{--}25\text{ cm}^{-1}$ , respectively. The improved performance of hybrid density functionals on vibrational properties of Mg silicates, supported by several dedicated studies in the literature (Prencipe et al., 2009; Demichelis et al., 2010; De La Pierre et al., 2011; De La Pierre and Belmonte, 2016), is thus also confirmed in this work.

The volume (or pressure) dependence of vibrational frequencies in the framework of QHA is defined by the mode Grüneisen parameters ( $\gamma_i$ ), which allow in turn the determination of fundamental thermodynamic properties such as thermal expansion and  $P$ – $V$ – $T$  equation of state (e.g., Belmonte, 2017). Ab initio mode Grüneisen parameters of Raman-active modes calculated in this work show an excellent agreement with the few spectroscopic data available from the literature in the pressure range from 0 to 20 GPa (Chopelas et al., 1994; Chopelas, 2000). As far as we know, there are no experimental data for IR spectra of Mg<sub>2</sub>SiO<sub>4</sub> ringwoodite at high-pressure conditions. A comparison between theoretical and experimental results is shown in Fig. 1 and Table S2. The calculated  $\gamma_i$  values for the two most intense Raman bands in the 790–796 and 830–836 cm<sup>−1</sup> frequency range are 1.4 and 1.1, respectively, compared to observed values of 1.3 and 0.9 (Chopelas et al., 1994). The predicted average mode Grüneisen parameter is  $\langle\gamma\rangle = 1.19$ , very close to the experimental value of 1.11 derived from high-pressure Raman spectra. By comparing different DFT simulations, although Raman frequencies change in terms of wavenumbers (see Table S2), their mode Grüneisen parameters turn out to be quite similar to each other. However, this is not the case for the IR-active and silent modes. The pressure dependences of some of the  $T_{1u}$  modes (for instance that in the 330–350 cm<sup>−1</sup> region) and some of the silent modes as well (e.g., the low-frequency  $T_{2u}$  mode) are sensibly different if B3LYP results are compared to other GGA calculations (Piekarz et al., 2002; Hernández et al., 2015). This is one of the reasons why marked differences are also observed in the computed values of volume thermal expansion coefficients (see Sect. 3.3 below). It is interesting to note, finally, that the width of the phonon band gap predicted in this work at  $\Gamma$  point is about 170 cm<sup>−1</sup> at  $P = 0$ , thus sensibly narrower than that obtained by previous ab initio LDA and GGA investigations (Yu and Wentzcovitch, 2006; Piekarz et al., 2002; Hernández et al., 2015). The splitting between upper and lower phonon bands increases up to 260 cm<sup>−1</sup> at  $P = 27$  GPa. This likely occurs because the highest-frequency  $A_{1g}$  and  $T_{2g}$  vibrational modes, which are mostly related to stretching of Si–O stiff bonds in tetrahedral sites, display a steep pressure gradient (see Fig. 1 and Table S2 in the Supplement). Therefore the high-frequency modes are affected by pressure more than the medium- and

low-frequency modes, as observed also by Yu and Wentzcovitch (2006).

### 3.2 Thermoelastic properties

Thermoelastic properties of insulating and fixed-composition crystalline phases can be defined solely by the statistical mechanics analysis of vibrational modes of the crystal lattice (Born and Huang, 1954). The key entity is represented by the  $\alpha K_T$  product, which can be derived from the Helmholtz free energy  $F(V, T)$  by applying the thermodynamic identity:

$$\alpha K_T = \left(\frac{\partial P}{\partial T}\right)_V = -\frac{\partial}{\partial V} \left[ \left(\frac{\partial F}{\partial T}\right)_V \right]_T, \quad (4)$$

where  $\alpha$  and  $K_T$  are the volume thermal expansion coefficient (usually referred to as thermal expansivity) and the isothermal bulk modulus, respectively. The statistical mechanics expression is the following (see Belmonte, 2017):

$$\alpha K_T(V, T) = \frac{R}{ZV} \sum_{\mathbf{q}, i=1}^{3n} \gamma_i(\mathbf{q}, V) \times e^{X_i(\mathbf{q}, V)} \left( \frac{X_i(\mathbf{q}, V)}{e^{X_i(\mathbf{q}, V)} - 1} \right)^2, \quad (5)$$

where  $R$  is the universal gas constant,  $Z$  is the number of unit formula in the unit cell,  $V$  is the molar volume, and  $\gamma_i(\mathbf{q}, V)$  and  $X_i(\mathbf{q}, V)$  are the mode Grüneisen parameter and the adimensional frequency of the  $i$ th vibrational mode, respectively, which both depend on the  $\mathbf{q}$  point sampling and the volume of the crystal. The adimensional frequency can be simply obtained by converting the vibrational frequency wavenumbers  $\nu_i(\mathbf{q}, V)$  in angular frequencies  $\omega_i(\mathbf{q}, V)$  via the speed of light in vacuum ( $c$ ), i.e.,  $\omega_i(\mathbf{q}, V) = (2\pi c) \times \nu_i(\mathbf{q}, V)$  and then applying

$$X_i(\mathbf{q}, V) = \frac{\hbar\omega_i(\mathbf{q}, V)}{kT}, \quad (6)$$

where  $\hbar$  and  $k$  are the Planck and Boltzmann constants, respectively. By following a fully analytical approach, once the values of  $\alpha K_T$  have been computed by Eq. (5), thermal expansivity  $\alpha_V$  at given  $P$ – $T$  conditions can be defined if the values of the isothermal bulk modulus  $K_T$  are also known.

First-principle Mie–Grüneisen equation of state (FPMG-EOS) allow us to define thermoelastic parameters (i.e.,  $K_T$  and  $K'_T$ ) by fitting ab initio  $P$ – $V$ – $T$  (or  $F$ – $V$ – $T$ ) data obtained from phonon dispersion calculations (see Belmonte, 2017, for details). The ab initio B3LYP results of  $K_T$ ,  $K'_T = \left(\frac{\partial K_T}{\partial P}\right)_T$ ,  $\left(\frac{\partial K_T}{\partial T}\right)_P$  and  $\left(\frac{\partial^2 K_T}{\partial P \partial T}\right)$  as computed in this work for Mg<sub>2</sub>SiO<sub>4</sub> ringwoodite are shown in Fig. 2 and Table 1. Static values have been obtained by fitting energy–volume data ( $E$ – $V$ ) with a third-order Birch–Murnaghan EOS.

Static values calculated in this work for bulk modulus (i.e.,  $K_0 = 184.3$  GPa) are in remarkable agreement with experimental results, with the observed isothermal values being

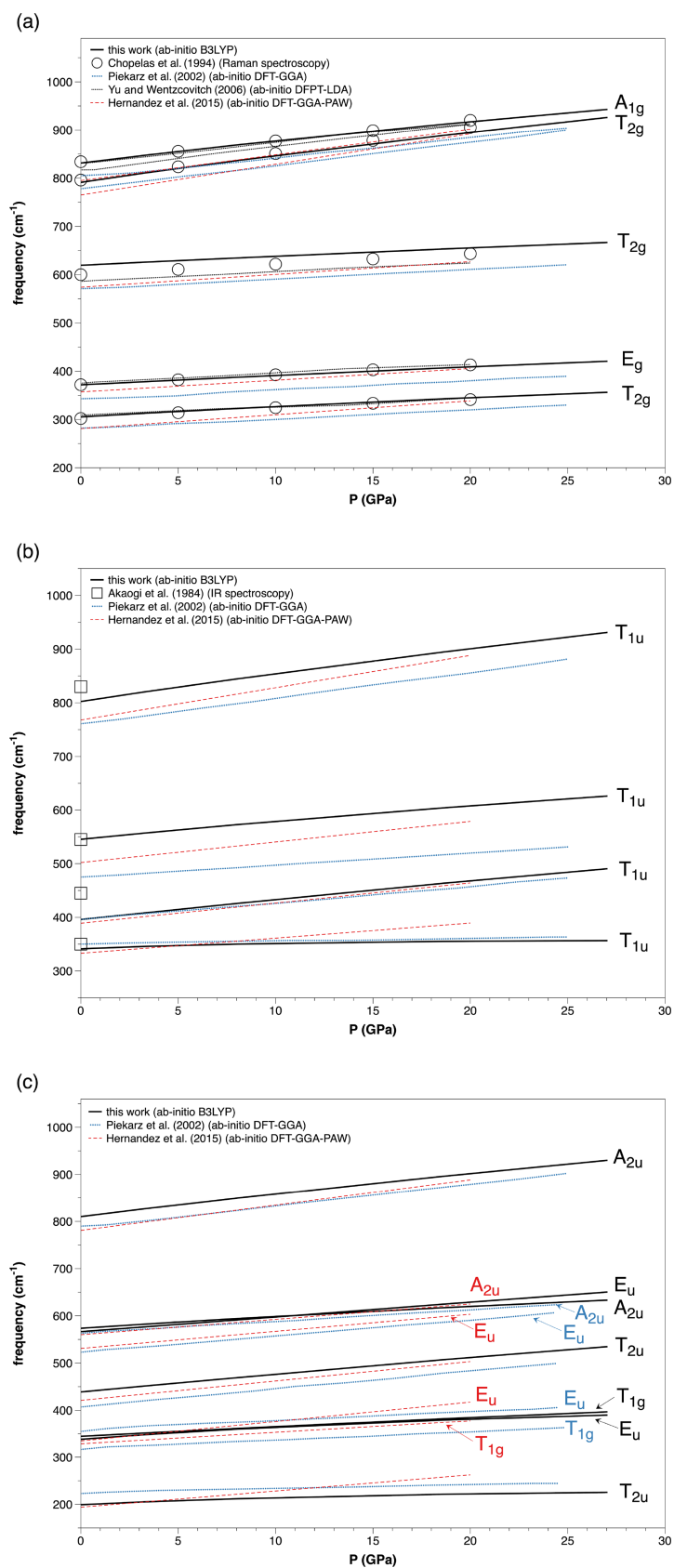


**Figure 1.** Pressure dependence of vibrational frequencies of  $\text{Mg}_2\text{SiO}_4$  ringwoodite. (a) Raman-active modes, (b) IR-active modes and (c) silent modes.

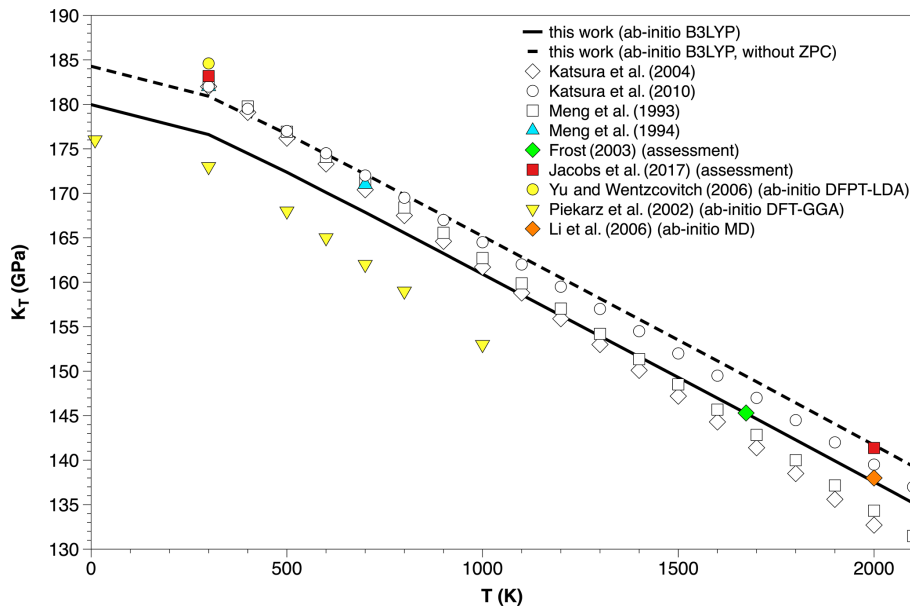


**Figure 2.** Temperature dependence of the isothermal bulk modulus ( $K_T$ ) of  $\text{Mg}_2\text{SiO}_4$  ringwoodite at zero or ambient pressure. Ab initio B3LYP results (with or without zero-point correction) are compared with available experimental data (Meng et al., 1993, 1994; Katsura et al., 2004, 2010), thermodynamic assessments (Frost, 2003; Jacobs et al., 2017) and previous ab initio DFT or MD simulations (Piekarz et al., 2002; Yu and Wentzcovitch, 2006; Li et al., 2006).

**Table 1.** Ab initio B3LYP thermal EOS parameters, as calculated in this work at  $P=0$  and different  $T$  conditions. Results obtained by experiments (M'94 – Meng et al., 1994; K'04 – Katsura et al., 2004; K'10 – Katsura et al., 2010), thermodynamic assessments (D'15 – Dorogokupets et al., 2015; J'17 – Jacobs et al., 2017) and different ab initio DFT (P'02 – Piekarz et al., 2002; YW'06 – Yu and Wentzcovitch, 2006) and first-principle molecular dynamics calculations (Li'06 – Li et al., 2006) are also shown.  $K_T$  is the isothermal bulk modulus (in GPa);  $K'_T$  and  $\left(\frac{\partial K_T}{\partial T}\right)_P$  are the first derivatives of  $K_T$  with respect to  $P$  and  $T$ , respectively;  $\left(\frac{\partial^2 K_T}{\partial P \partial T}\right)_0$  is the mixed  $P$ – $T$  derivative of  $K_T$  at  $T = 298.15$  K.

	This work (B3LYP)	M'94 (Exp.)	K'04 (Exp.)	K'10 (Exp.)	D'15 (Calc.)	J'17 (Calc.)	P'02 (GGA)	Li'06 (FPMD)
$K_0$ (0 K)	184.3 <sup>a</sup> 180.0 <sup>b</sup>	–	–	–	–	183.67 <sup>a</sup> 186.06 <sup>b</sup>	176	176
$K_T$ (300 K)	176.6	182(3)	182.0 <sup>d</sup>	182.0	187.4	183.18	173	–
$K'_T$ (0 K)	4.13	–	–	–	–	4.21(17)	–	4.07
$K'_T$ (300 K)	4.16	4.2(3)	4.6(2)	4.8(2)	3.98	–	–	–
$\left(\frac{\partial K_T}{\partial T}\right)_P$ (GPa K <sup>-1</sup> )	–0.0233	–0.027(3)	–0.029(1)	–0.025(1)	–0.0236 <sup>c</sup>	–0.0246 <sup>c</sup>	–0.0288 <sup>c</sup>	–0.022(3) <sup>c</sup>
$\left(\frac{\partial^2 K_T}{\partial P \partial T}\right)_0$ ( $\times 10^{-4}$ K <sup>-1</sup> )	1.0	5.5 $\pm$ 5.2	–	–	0.9	–	–	6.6 $\pm$ 1.8 <sup>c</sup>

<sup>a</sup> Static values. <sup>b</sup> Values at  $T = 0$  K including zero-point correction (ZPC). <sup>c</sup> Results given by linear fitting of published data. <sup>d</sup> Fixed value.

around 182–185 GPa at ambient conditions (Hazen, 1993; Meng et al., 1994; Katsura et al., 2004, 2010; see also Table 1). On the other hand, literature values of  $K'_0$  seem to be more scattered, ranging from 4.2 up to almost 5.0. Our calculated values for the bulk modulus pressure derivative (i.e.,  $K'_0 = 4.13$  at the static level,  $K'_{T,300} = 4.16$  at  $T = 300$  K and ambient pressure) are much closer to the experimental val-

ues of Meng et al. (1994) and to some vibrationally constrained thermodynamic assessments as well (e.g., Jacobs et al., 2017) (Table 1). A thorough comparison between different ab initio DFT simulations shows that B3LYP results are intermediate between those obtained by LDA and GGA, respectively, as expected from previous theoretical studies on the elasticity and EOS of several high-pressure minerals with

hybrid density functionals (e.g., Erba et al., 2014; Prencipe et al., 2014; Ulian and Valdrè, 2018). In particular, LDA calculations give an upper bound to the calculated static or room-temperature bulk moduli, yielding values in the range 184–208 GPa (Kiefer et al., 1997, 1999; Yu and Wentzcovitch, 2006; Panero, 2008; Núñez-Valdez et al., 2011), while a lower bound of 175–178 GPa is provided by GGA-based DFT or MD simulations (Piekarz et al., 2002; Li et al., 2006, 2009; Panero, 2008; Hernández et al., 2015). It is interesting to note that vibrational effects on EOS parameters are relevant as  $K_T$  and  $K'_T$  at  $T = 300$  K are rather different from static values. The former is lowered by  $\sim 8$  GPa (i.e., about 4%), and the latter increases from 4.13 to 4.16 (Table 1). The effect of zero-point motions alone decreases the bulk modulus by  $\sim 2.5\%$  over the entire temperature range (see Fig. 2). Those outcomes on ringwoodite are thus consistent with that observed for other high-pressure Mg silicates, like for instance bridgmanite (Oganov et al., 2001), suggesting that vibrational effects on thermoelastic properties cannot be disregarded in DFT simulations even at ambient  $P$ – $T$  conditions (see Belmonte, 2017).

The temperature dependence of the isothermal bulk modulus of  $\text{Mg}_2\text{SiO}_4$  ringwoodite at  $P = 0$  GPa is shown in Fig. 2. Ab initio B3LYP results compare favorably with literature values, especially in the medium- to high-temperature range. The value inferred for  $\left(\frac{\partial K_T}{\partial T}\right)_P$  by linear fitting of ab initio data is  $-0.0233 \text{ GPa K}^{-1}$ , which is not far from the available experimental results (Meng et al., 1993, 1994; Katsura et al., 2010). The only exception is represented by the markedly negative value given by Katsura et al. (2004) (see Table 1). Interestingly, the computed  $\left(\frac{\partial K_T}{\partial T}\right)_P$  is in excellent agreement with that obtained by some thermodynamic assessments based on the Helmholtz free energy, hence constrained by vibrational theory (Dorogokupets et al., 2015; Jacobs et al., 2017). Furthermore, the isothermal bulk modulus values computed by ab initio B3LYP at HT conditions are nearly coincident with those predicted by Frost (2003) at  $T = 1673$  K and by the ab initio MD simulation of Li et al. (2006) at  $T = 2000$  K (see Fig. 2). For instance, Li et al. (2006) obtain  $K_T = 138 \pm 6$  GPa at  $T = 2000$  K, compared to our value of 137.6 GPa at the same temperature. This remarkable agreement supports the evidence that QHA performs well for  $\text{Mg}_2\text{SiO}_4$  ringwoodite in the whole  $P$ – $T$  range of the mantle transition zone. Conversely, other “internally consistent” thermodynamic assessments give  $K_T$  values for ringwoodite which are overestimated (Holland and Powell, 2011) or possibly affected by physical unsoundness (Fabrichnaya et al., 2004).

The mixed  $P$ – $T$  derivative of the isothermal bulk modulus has also been constrained in this work. Ab initio B3LYP calculations give  $\left(\frac{\partial^2 K_T}{\partial P \partial T}\right)_0 \cong 1.0 \times 10^{-4} \text{ K}^{-1}$  at room temperature, which is virtually identical to the assessed value by Dorogokupets et al. (2015) and in qualitative agreement

with the experimental results of Meng et al. (1994) within their quite large uncertainties (see Table 1). First-principle MD simulations of Li et al. (2006) provide a higher  $K'_T$  of  $5.2 \pm 0.3$  at  $T = 2000$  K (against  $K'_{T,2000} = 4.33$  predicted in this work), but also in this case the agreement seems to be reasonable in view of the huge uncertainties which currently affect the definition of thermoelastic properties of deep mantle minerals at simultaneous high-pressure and high-temperature conditions.

### 3.3 Thermal expansion and thermal expansivity

It is well known that hybrid functionals like B3LYP, which are based on the generalized gradient approximation for the DFT exchange–correlation term, overestimate molar volumes of magnesium silicates by  $\sim 1\%$ – $2\%$ , essentially due to an underbinding trend predicted for Mg–O and Si–O bond lengths (Kohanoff, 2006; Ottonello et al., 2009; Belmonte et al., 2014). The optimized unit cell volume of ringwoodite at the athermal limit (i.e.,  $T = 0$  K,  $P = 0$  GPa) is  $V_0 = 530.9 \text{ \AA}^3$ , that is 1% higher than experimental values obtained by X-ray diffraction at ambient conditions (Sasaki et al., 1982; Katsura et al., 2004). Nevertheless, zero-pressure relative volume thermal expansion (i.e.,  $V/V_0$ ) and thermal expansivity ( $\alpha_V$ ) are accurately reproduced in the framework of QHA up to a limit, which, as a rule of thumb, lies within the Debye temperature and two-thirds of the melting point of the substance. This limit is purely empirical in nature and may change according to the physicochemical properties of the solid phase. In other words, deviations from the observed trend may occur due to the onset of anharmonic effects at temperature conditions not so far from the melting point. In such a case, the crystalline substance can be referred to as a “quasi-harmonic” solid. Ab initio B3LYP results of volume thermal expansion and thermal expansivity are shown in Figs. 3 and 4, respectively.

The values of  $\alpha_V$  computed at zero pressure and discrete temperatures by the statistical thermodynamic approach described in Sect. 3.2 are fitted by a suitable polynomial function in the temperature range from  $T_r = 298.15$  K to  $T = 2000$  K, as follows:

$$\alpha_V(P_0, T) = \alpha_0 + \alpha_1 T + \alpha_2 T^{-1} + \alpha_3 T^{-2} + \alpha_4 T^{-3}. \quad (7)$$

Fitted numerical coefficients of the polynomial function at  $P = 0$  are  $\alpha_0 = 1.6033 \times 10^{-5} \text{ K}^{-1}$ ,  $\alpha_1 = 8.839 \times 10^{-9} \text{ K}^{-2}$ ,  $\alpha_2 = 11.586 \times 10^{-3}$ ,  $\alpha_3 = -6.055 \text{ K}$  and  $\alpha_4 = 804.31 \text{ K}^2$  (see Table 2). Relative volume thermal expansion can thus be obtained by analytical integration of  $\alpha_V$ , i.e.,

$$\frac{V}{V_0}(P_0, T) = \exp \int_{T_r}^T \alpha_V(P_0, T) dT. \quad (8)$$

A huge uncertainty exists on the ambient value of volume thermal expansion coefficient of  $\text{Mg}_2\text{SiO}_4$  ring-

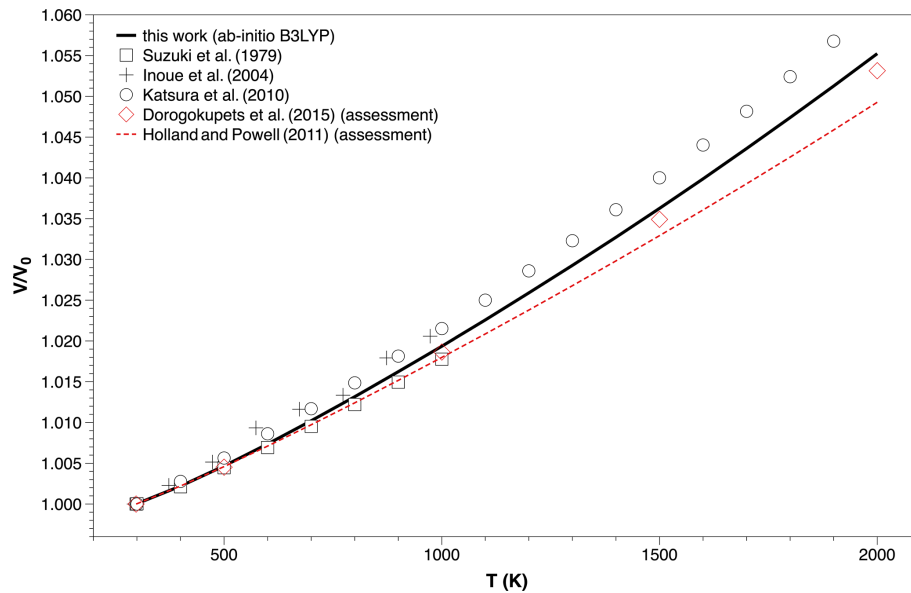


**Figure 3.** Ab initio B3LYP volume thermal expansion ( $V/V_0$ ) of  $\text{Mg}_2\text{SiO}_4$  ringwoodite at zero pressure, compared with experimental data (Suzuki et al., 1979; Inoue et al., 2004; Katsura et al., 2010) and thermodynamic assessments (Holland and Powell, 2011; Dorogokupets et al., 2015) at ambient pressure.

woodite (Nestola, 2016), with experimental values ranging from  $\alpha_{V_0} = 1.51 \times 10^{-5} \text{ K}^{-1}$  (Ming et al., 1992) to  $\alpha_{V_0} = 3.07 \times 10^{-5} \text{ K}^{-1}$  (Inoue et al., 2004).  $\alpha_{V_0}$  can thus vary as much as 100% according to different experimental investigations. The computed value in this work, i.e.,  $\alpha_{V_0} = 1.98 \times 10^{-5} \text{ K}^{-1}$ , is not far from the experimental value  $\alpha_{V_0} = (1.86 \pm 0.09) \times 10^{-5} \text{ K}^{-1}$  obtained by Suzuki et al. (1979). Both values are quite different from those determined by other experimental works (Meng et al., 1994; Katsura et al., 2004). Again, ambient thermal expansion coefficients calculated by lattice dynamics modeling or other vibrationally constrained assessments are in remarkable agreement with our result (i.e.,  $\alpha_{V_0} = 1.84 \pm 0.10 \times 10^{-5} \text{ K}^{-1}$  according to Chopelas, 2000;  $\alpha_{V_0} = 1.89 \times 10^{-5} \text{ K}^{-1}$ , Dorogokupets et al., 2015;  $\alpha_{V_0} = 1.99 \times 10^{-5} \text{ K}^{-1}$ , Jacobs et al., 2017). This result can be interpreted as a clear sign of thermodynamic soundness of thermal expansion data.

The calculated trend of volume thermal expansion up to high-temperature conditions provides some insights into the thermodynamic behavior of ringwoodite at deep mantle conditions (Figs. 3 and 4). Ab initio thermal expansivity as calculated in this work is relatively different from the HT extrapolation of experimental data (see Fig. 4a). In particular, B3LYP gives  $\alpha_V$  values which are higher than those determined by Suzuki et al. (1979) at  $T > 1000 \text{ K}$  but much lower than the observed trend by Katsura et al. (2004). However, the optimized trend of Katsura et al. (2010) is in excellent agreement with our calculations in the whole temperature range, except for the ambient value (i.e.,  $\alpha_{V_0} = 2.45 \pm 0.05 \times 10^{-5} \text{ K}^{-1}$ ), which seems to be strongly overestimated with respect to our result and to

**Table 2.** Ab initio B3LYP thermal expansivity of  $\text{Mg}_2\text{SiO}_4$  ringwoodite up to mantle transition zone conditions ( $\alpha_V$  in  $\text{K}^{-1}$ ). Fitted coefficients of the function  $\alpha_V(P, T) = (\alpha_0 + \alpha_1 T + \alpha_2 T^{-1} + \alpha_3 T^{-2} + \alpha_4 T^{-3}) \exp(-\alpha_5 P)$  are valid in the  $P$ - $T$  range between 0–25 GPa and 298.15–2000 K.

$\alpha_V$	Ab initio B3LYP
$\alpha_0 \times 10^5 (\text{K}^{-1})$	1.6033
$\alpha_1 \times 10^9 (\text{K}^{-2})$	8.839
$\alpha_2 \times 10^3$	11.586
$\alpha_3 (\text{K})$	−6.055
$\alpha_4 (\text{K}^2)$	804.31
$\alpha_5 \times 10^2 (\text{GPa}^{-1})$	2.52

that observed by Suzuki et al. (1979) as well. This leads in turn to a different trend in the relative volume thermal expansion (Fig. 3). The evidence that different DFT and QHA simulations give quite similar values of  $\alpha_{V_0}$  (see Piekarcz et al., 2002; Yu and Wentzcovitch, 2006; Hernández et al., 2015) strengthens the ability of ab initio calculations to identify and select accurate experimental results for thermal expansivity. For instance, the  $\alpha_V$  values determined by Ming et al. (1992) are likely affected by severe underestimation (Fig. 4a). On the other hand, the temperature dependence of thermal expansivity may change among different theoretical simulations. Ab initio B3LYP gives  $\left(\frac{\partial \alpha_V}{\partial T}\right)_{P_0}$  similar to those calculated by Chopelas (2000) and Dorogokupets et al. (2015), but sensibly different from that obtained by other ab initio DFT-GGA calculations (Piekarcz et al., 2002) (see Fig. 4b).

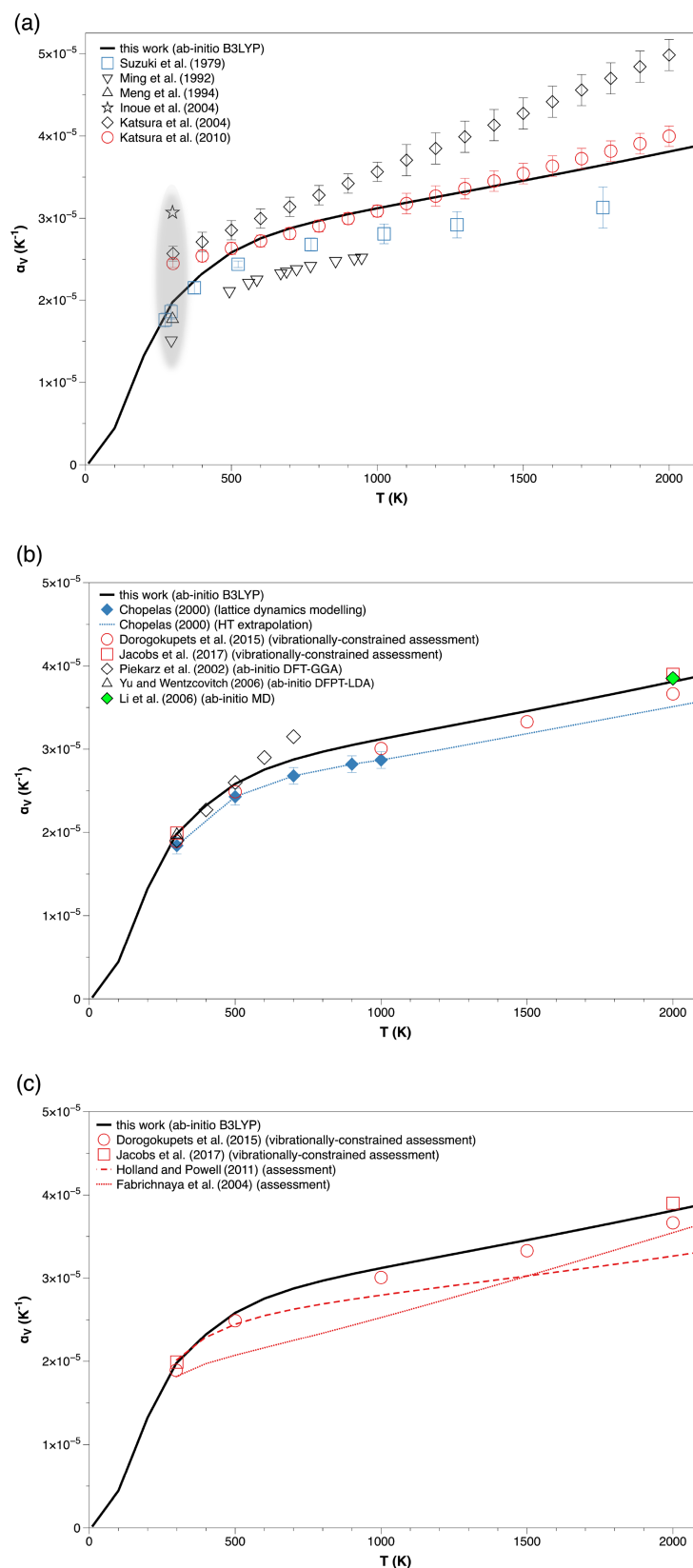


**Figure 4.** Ab initio B3LYP volume thermal expansivity ( $\alpha_V$ ) of  $\text{Mg}_2\text{SiO}_4$  ringwoodite at zero pressure, compared with (a) experimental data (grey shaded area highlights scattering of values at ambient conditions), (b) different theoretical simulations and (c) thermodynamic assessments.

Interestingly,  $\alpha_V$  does not display any inflection point in the entire  $T$  range investigated in this work, thus confirming that (i) QHA performs exceptionally well for  $\text{Mg}_2\text{SiO}_4$  ringwoodite up to deep mantle temperatures and (ii) ringwoodite can be considered a “quasi-harmonic” solid in the Earth’s mantle transition zone. Further supporting evidence is that the thermal expansivity predicted at  $T = 2000$  K and room pressure by the first-principle molecular dynamics of Li et al. (2006) are almost identical to that predicted by this work, with the former being equal to  $3.85 \times 10^{-5} \text{ K}^{-1}$  and the latter around  $3.81 \times 10^{-5} \text{ K}^{-1}$  (Fig. 4b). This confirms the performance of ab initio B3LYP and QHA calculations since MD simulations, which are able to catch anharmonic effects, give nearly coincident results on thermal expansivity in the high-temperature range. Therefore, intrinsic anharmonic effects do seem to be negligible for  $\text{Mg}_2\text{SiO}_4$  ringwoodite even at HT (and low-pressure) conditions.

The comparison between ab initio calculations and internally consistent thermodynamic assessments deserves special attention. Figure 4c shows that thermal expansivity assessed via mathematical procedures able to reproduce selected phase equilibria of  $\text{Mg}_2\text{SiO}_4$  ringwoodite (e.g., Fabrichnaya et al., 2004; Holland and Powell, 2011) turns out to be inaccurate at mantle temperatures. For instance, Holland and Powell (2011) used a thermal pressure Tait EOS, along with some assumptions on thermoelastic properties, to predict thermal expansion of mantle minerals at HP–HT conditions.  $\alpha_V$  values obtained for  $\text{Mg}_2\text{SiO}_4$  ringwoodite are underestimated by 10 %–15 % in the high-temperature range (see Fig. 4c). The same also applies to the relative volume thermal expansion trend depicted in Fig. 3. This is perhaps even more evident if thermal expansion data by Fabrichnaya et al. (2004) are considered in Fig. 4c, which basically means that internally consistent thermodynamic datasets currently developed for deep mantle minerals are not necessarily also physically consistent. In this respect, it does not seem fortuitous that thermodynamic assessments based on Helmholtz free energy and/or constrained by vibrational theory (e.g., Dorogokupets et al., 2015; Jacobs et al., 2017) provide thermal expansion data very close to the ab initio results obtained in this work (Figs. 3 and 4c).

The coupling between thermal expansivity and isothermal bulk modulus provides a further clue on the physical soundness of thermoelastic properties and the robustness of their extrapolation to deep mantle temperatures. This is not a trivial task from an experimental point of view, since  $\alpha K_T$  values are difficult to be constrained at those conditions. Kojitani et al. (2016) tried to infer  $K_T$  of  $\text{Mg}_2\text{SiO}_4$  ringwoodite by fitting experimental  $P$ – $V$ – $T$  data of Katsura et al. (2004) with a high-temperature third-order Birch–Murnaghan EOS and by assuming  $\alpha_V$  of Suzuki et al. (1979) as fixed in the fitting. They obtain  $\left(\frac{\partial K_T}{\partial T}\right)_P = -0.019(3) \text{ GPa K}^{-1}$ , which is much less negative than any other theoretical or experimental determinations (see Table 1). This is most likely

due to the fact that the two experimental datasets cannot be reconciled by the assessment. Ottonello et al. (2009) obtain a value of  $\left(\frac{\partial K_T}{\partial T}\right)_P = -0.0104 \text{ GPa K}^{-1}$ , which is even less negative and leads to an overestimation of  $K_T$  values of ringwoodite at HT. In that case, an overestimation may occur because the assessment of thermoelastic properties is not based on the full vDOS but rather on a semi-classical thermodynamic approximation employing the logarithmic volume derivative of the Grüneisen parameter (the so-called  $q^{ht}$  parameter), which is difficult to constrain by lattice dynamics calculations (Anderson, 1995). The average value of the  $\alpha K_T$  product calculated for mantle phases over an appropriate temperature range can give useful insights into the accuracy of thermoelastic data (Stixrude and Lithgow-Bertelloni, 2005). If we consider the average value of  $\alpha K_T$  of  $\text{Mg}_2\text{SiO}_4$  ringwoodite over a  $T$  range from 300 to 1000 K, namely where the temperature gradient of  $\alpha_V$  is steeper, we obtain  $45.6 \text{ bar K}^{-1}$  according to our calculations. Vibrationally constrained thermodynamic assessments (e.g., Stixrude and Lithgow-Bertelloni, 2005) give values around  $44 \text{ bar K}^{-1}$ , in excellent agreement with the ab initio value determined by Eq. (4), while other internally consistent thermodynamic databases could give clearly inaccurate results (e.g.,  $\bar{\alpha} K_{T300-1000 \text{ K}} = 37.3 \text{ bar K}^{-1}$  according to Fabrichnaya et al., 2004). As for experimental data, there is a marked difference between the dataset of Katsura et al. (2004) and that of Katsura et al. (2010), with the latter being much closer to ab initio results than the former (i.e.,  $\bar{\alpha} K_{T300-1000 \text{ K}} = 52.7$  and  $48.0 \text{ bar K}^{-1}$ , respectively). This confirms the predictive power of state-of-the-art ab initio calculations in constraining the extrapolation of experimental data at deep mantle conditions.

#### 4 Implications: thermal expansivity at mantle transition zone conditions

Thermal expansivity is a key parameter for mantle dynamics. Buoyancy forces that control thermal convection in the Earth’s mantle are driven by lateral variations in temperature and density, which are in turn determined by the local volume thermal expansion of the constituent mineral phases (Christensen and Yuen, 1985). Thermal expansivity is commonly assumed as either constant or simply pressure-dependent by most numerical simulations of mantle convection, while simultaneous  $P$ – $T$  dependence is only rarely taken into account (Schmeling et al., 2003; Tosi et al., 2013).

In this work,  $\alpha_V(P, T)$  and  $K_T(P, T)$  functions of  $\text{Mg}_2\text{SiO}_4$  ringwoodite are computed in a broad range of  $P$ – $T$  conditions compatible with the stability of this phase in the Earth’s mantle transition zone (i.e.,  $P = 0$ – $25$  GPa,  $T = 298.15$ – $2000$  K). The following six-parameter analytical function is able to reproduce ab initio values in the whole investigated  $P$ – $T$  range with a maximum deviation of a few percent:

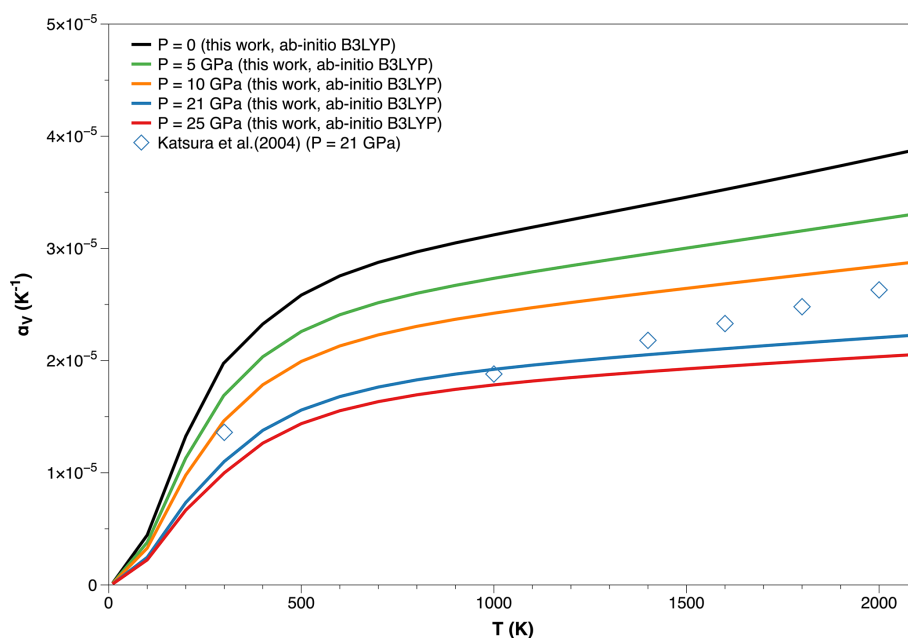


**Figure 5.** Ab initio volume thermal expansivity ( $\alpha_V$ ) of  $\text{Mg}_2\text{SiO}_4$  ringwoodite at different pressures ( $P = 0, 5, 10, 21$  and  $25$  GPa). Experimental data at  $P = 21$  GPa are from Katsura et al. (2004).

$$\alpha_V(P, T) = \left( \alpha_0 + \alpha_1 T + \alpha_2 T^{-1} + \alpha_3 T^{-2} + \alpha_4 T^{-3} \right) \times \exp(-\alpha_5 P), \quad (9)$$

and therefore it has been adopted in this work. The coefficient  $\alpha_5$  in Eq. (9) has been fitted starting from the polynomial function at  $P = 0$  (see Eq. 7), and then applying an exponential pressure dependence (Table 2). A similar parametrization was also implemented by Tosi et al. (2013) in their numerical modeling of mantle convection due to its relatively simple form.

Figure 5 shows ab initio B3LYP thermal expansivity calculated at different pressure conditions (i.e.,  $P = 0, 5, 10, 21$  and  $25$  GPa).  $\alpha_V(P, T)$  is strongly pressure-dependent and does not show any inflection point in the whole  $P$ – $T$  range investigated in this work, thus supporting again the quasi-harmonic nature of ringwoodite at mantle transition zone conditions. The experimental values obtained by Katsura et al. (2004) at  $P = 21$  GPa are in qualitative agreement with our calculations up to about 1000 K and then deviate at higher temperatures. Even though experimental uncertainties in  $\alpha_V$  values are not provided at  $P = 21$  GPa, overestimation of room-temperature  $\alpha_V$  seems to also be kept at high pressures.

Even more interesting is the analysis of ab initio volume thermal expansion calculated up to mantle transition zone pressures along different isotherms (i.e.,  $T = 500, 1000, 1500$  and  $2000$  K) (Fig. 6). By the computed trends in Fig. 6 it is quite evident that the pressure dependence of volume thermal expansion of ringwoodite becomes more marked with

increasing temperature. This means that inaccurate extrapolations of low-pressure data at mantle transition zone conditions could lead to large errors in predicted molar volume and density values at HP–HT, thus affecting phase equilibrium calculations and large-scale numerical modeling of mantle convection at those conditions. Experimental values obtained by in situ X-ray diffraction in a multianvil apparatus by Katsura et al. (2004), although sensibly scattered, turn out to be in good agreement with ab initio results. The combined  $P$ – $T$  effects on thermal expansivity of ringwoodite are shown by a contour plot in Fig. 7, which displays calculated  $\alpha_V(P, T)$  values within the stability field of the spinel-structured  $\text{Mg}_2\text{SiO}_4$  polymorph at depths of the lower mantle transition zone (i.e.,  $> 520$  km) as inferred by global geophysical models (Dziewonski and Anderson, 1981; Brown and Shankland, 1981). Since contour lines change their slope going from shallow to deep MTZ conditions, the increased pressure dependence of thermal expansivity with temperature is highlighted even more clearly. Ab initio DFT–QHA simulations thus provide a fundamental constraint to interpret deep mantle processes under a mineral physics and thermodynamic perspective.

## 5 Conclusions

We showed that modern DFT–QHA calculations with the hybrid functional B3LYP are able to accurately predict volume thermal expansion and thermoelastic properties of  $\text{Mg}_2\text{SiO}_4$  ringwoodite up to mantle transition zone conditions. Ab initio results of  $\alpha_V(P, T)$ ,  $V/V_0(P, T)$  and  $K_T(P, T)$  give a

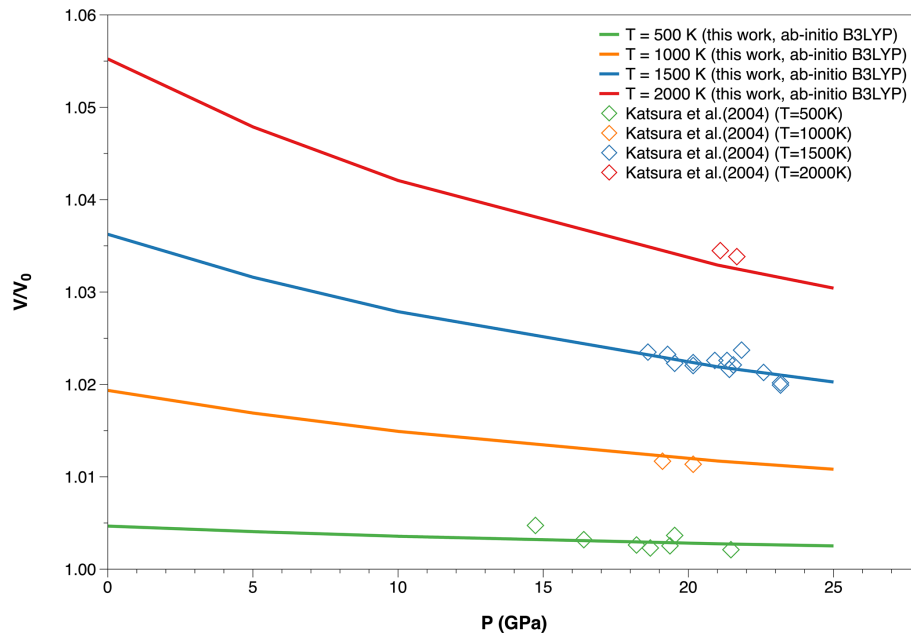


**Figure 6.** Ab initio volume thermal expansion ( $V/V_0$ ) of  $\text{Mg}_2\text{SiO}_4$  ringwoodite along different isotherms ( $T = 500, 1000, 1500$  and  $2000$  K). Experimental data are taken from Katsura et al. (2004).

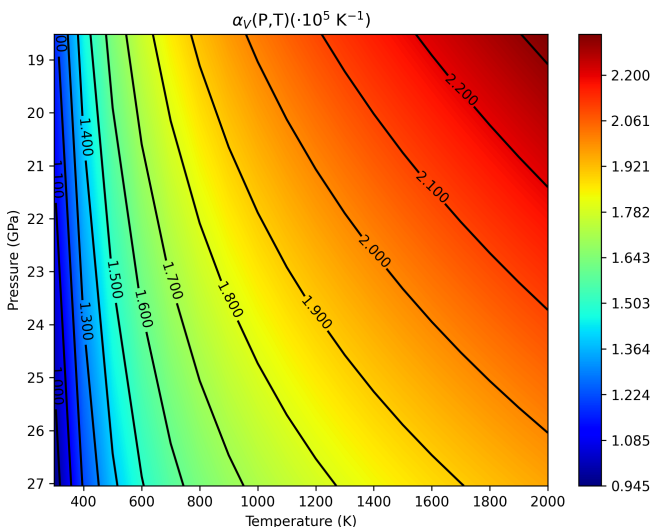


**Figure 7.** Contour plot of ab initio volume thermal expansivity  $\alpha_V(P, T)$  of  $\text{Mg}_2\text{SiO}_4$  ringwoodite at mantle transition zone conditions.

physical constraint to the HP–HT extrapolation of thermoelastic properties as determined by laboratory experiments, thus enhancing our understanding of mantle processes (e.g., thermal convection) in planetary interiors. Theoretical analysis of lattice dynamics allowed the interpretation of vibrational spectra at both ambient and high-pressure conditions by suggesting that IR-active and silent modes, along with their mode Grüneisen parameters, play a key role in determining volume thermal expansion of ringwoodite, particu-

larly at high temperatures and pressures. Since literature data on those vibrational modes are still scarce or controversial, the huge uncertainties that currently affect thermal expansivity of this mantle mineral may be readily understood. In this respect, vibrationally constrained thermoelastic properties as computed by ab initio methods revealed that physical unsoundness could be concealed under internally consistent thermodynamic datasets developed for mantle phases. Ab initio thermal expansivity and isothermal bulk modulus calculated in this work in a broad range of  $P$ – $T$  conditions (i.e.,  $P = 0$ – $25$  GPa,  $T = 0$ – $2000$  K) support the evidence of a quasi-harmonic behavior of ringwoodite in the Earth’s mantle transition zone. In fact, high-temperature values of  $\alpha_V$  and  $K_T$  predicted in this work by DFT–QHA calculations turn out to be nearly coincident with the results of the first-principle molecular dynamics simulation by Li et al. (2006), stressing that intrinsic anharmonic effects are virtually absent at MTZ conditions. Finally, since thermal expansivity of  $\text{Mg}_2\text{SiO}_4$  ringwoodite is strongly pressure-dependent and its pressure dependence increases with increasing temperature (see Figs. 5–7), extrapolation of low-pressure thermoelastic data to deep mantle conditions should be taken with care to avoid inaccurate or spurious numerical predictions.

*Data availability.* All data derived from this research are presented in the main text, enclosed tables and figures, and Supplement.

*Supplement.* The supplement related to this article is available online at: <https://doi.org/10.5194/ejm-34-167-2022-supplement>.

*Author contributions.* DB designed the research, performed the calculations and wrote the paper. DB, MLF and FM worked on data interpretation, discussed the results and commented on the paper.

*Competing interests.* The contact author has declared that neither they nor their co-authors have any competing interests.

*Disclaimer.* Publisher's note: Copernicus Publications remains neutral with regard to jurisdictional claims in published maps and institutional affiliations.

*Special issue statement.* This article is part of the special issue "Probing the Earth: experiments and mineral physics at mantle depths". It is not associated with a conference.

*Acknowledgements.* Financial support by the Italian MIUR PRIN 2017 (project number: 2017KY5ZX8) is warmly acknowledged. We also acknowledge the CINECA award under the ISCRA initiative (ISCRA C Project THOMMY, HP10CNF2NR), for the availability of high-performance-computing resources and support.

*Financial support.* This research has been supported by the Ministero dell'Istruzione, dell'Università e della Ricerca (grant no. MIUR PRIN 2017 – project 2017KY5ZX8).

*Review statement.* This paper was edited by Monika Koch-Müller and reviewed by two anonymous referees.

## References

- Acosta-Maeda, T. E., Scott, E. R. D., Sharma, S. K., and Misra, A. K.: The pressures and temperatures of meteorite impact: evidence from micro-Raman mapping of mineral phases in the strongly shocked Taiban ordinary chondrite, *Am. Mineral.*, 98, 859–869, <https://doi.org/10.2138/am.2013.4300>, 2013.
- Akaogi, M., Ross, N. L., McMillan, P., and Navrotsky, A.: The Mg<sub>2</sub>SiO<sub>4</sub> polymorphs (olivine, modified spinel and spinel) – thermodynamic properties from oxide melt solution calorimetry, phase relations, and models of lattice vibrations, *Am. Mineral.*, 69, 499–512, 1984.
- Akaogi, M., Takayama, H., Kojitani, H., Kawaji, H., and Atake, T.: Low-temperature heat capacities, entropies and enthalpies of Mg<sub>2</sub>SiO<sub>4</sub> polymorphs, and  $\alpha$ - $\beta$ - $\gamma$  and post-spinel phase relations at high pressure, *Phys. Chem. Miner.*, 34, 169–183, <https://doi.org/10.1007/s00269-006-0137-3>, 2007.
- Anderson, O. L.: *Equations of State of Solids for Geophysics and Ceramic Science*, Oxford Monographs on Geology and Geophysics No. 31, Oxford University Press, New York, ISBN 9780195056068, 1995.
- Bass, J. D. and Anderson, D. L.: Composition of the upper mantle: geophysical tests of two petrological models, *Geophys. Res. Lett.*, 11, 237–240, <https://doi.org/10.1029/GL011i003p00229>, 1984.
- Becke, A. D.: Density-functional thermochemistry. III. The role of exact exchange, *J. Chem. Phys.*, 98, 5648–5652, <https://doi.org/10.1063/1.464913>, 1993.
- Belmonte, D.: First principles thermodynamics of minerals at HP-HT conditions: MgO as a prototypical material, *Minerals*, 7, 183, <https://doi.org/10.3390/min7100183>, 2017.
- Belmonte, D., Ottonello, G., and Vetuschi Zuccolini, M.: Melting of  $\alpha$ -Al<sub>2</sub>O<sub>3</sub> and vitrification of the undercooled alumina liquid: ab initio vibrational calculations and their thermodynamic implications, *J. Chem. Phys.*, 138, 064507, <https://doi.org/10.1063/1.4790612>, 2013.
- Belmonte, D., Ottonello, G., and Vetuschi Zuccolini, M.: Ab initio thermodynamic and thermophysical properties of sapphirine end-members in the join Mg<sub>4</sub>Al<sub>8</sub>Si<sub>2</sub>O<sub>20</sub>-Mg<sub>3</sub>Al<sub>10</sub>SiO<sub>20</sub>, *Am. Mineral.*, 99, 1449–1461, <https://doi.org/10.2138/am.2014.4833>, 2014.
- Belmonte, D., Gatti, C., Ottonello, G., Richet, P., and Vetuschi Zuccolini, M.: Ab initio thermodynamic and thermophysical properties of sodium metasilicate, Na<sub>2</sub>SiO<sub>3</sub>, and their electron-density and electron-pair-density counterparts, *J. Phys. Chem. A*, 120, 8881–8895, <https://doi.org/10.1021/acs.jpca.6b08676>, 2016.
- Belmonte, D., Ottonello, G., and Vetuschi Zuccolini, M.: The system MgO-Al<sub>2</sub>O<sub>3</sub>-SiO<sub>2</sub> under pressure: a computational study of melting relations and phase diagrams, *Chem. Geol.*, 461, 54–64, <https://doi.org/10.1016/j.chemgeo.2016.11.011>, 2017a.
- Belmonte, D., Ottonello, G., and Vetuschi Zuccolini, M.: Ab initio-assisted assessment of the CaO-SiO<sub>2</sub> system under pressure, *CALPHAD*, 59, 12–30, <https://doi.org/10.1016/j.calphad.2017.07.009>, 2017b.
- Bina, C. R. and Helffrich, G.: Phase transition Clapeyron slopes and transition zone seismic discontinuity topography, *J. Geophys. Res.-Sol. Ea.*, 99, 15853–15860, <https://doi.org/10.1029/94JB00462>, 1994.
- Bindi, L., Griffin, W. L., Panero, W. R., Sirotkina, E., Bobrov, A., and Irifune, T.: Synthesis of inverse ringwoodite sheds light on the subduction history of Tibetan ophiolites, *Sci. Rep.*, 8, 5457, <https://doi.org/10.1038/s41598-018-23790-9>, 2018.
- Born, M. and Huang, K.: *Dynamical Theory of Crystal Lattices*, Oxford University Press, Oxford, UK, ISBN 9780198503699, 1954.
- Brown, J. M. and Shankland, T. J.: Thermodynamic parameters in the Earth as determined from seismic profiles, *Geophys. J. Int.*, 66, 579–596, <https://doi.org/10.1111/j.1365-246X.1981.tb04891.x>, 1981.
- Chen, M., El Goresy, A., and Gillet, P.: Ringwoodite lamellae in olivine: clues to olivine-ringwoodite phase transition mechanisms in shocked meteorites and subducting slabs, *P. Natl. Acad. Sci. USA*, 101, 15033–15037, <https://doi.org/10.1073/pnas.0405048101>, 2004.
- Chopelas, A.: Thermal expansivity of mantle relevant magnesium silicates derived from vibrational spectroscopy at high pressure, *Am. Mineral.*, 85, 270–278, <https://doi.org/10.2138/am-2000-2-301>, 2000.

- Chopelas, A., Boehler, R., and Ko, T.: Thermodynamics and behavior of  $\gamma$ - $\text{Mg}_2\text{SiO}_4$  at high pressure: implications for  $\text{Mg}_2\text{SiO}_4$  phase equilibrium, *Phys. Chem. Miner.*, 21, 351–359, <https://doi.org/10.1007/BF00203293>, 1994.
- Christensen, U. and Yuen, D. A.: Layered convection induced by phase transitions, *J. Geophys. Res.-Sol. Ea.*, 90, 10291–10300, <https://doi.org/10.1029/jb090ib12p10291>, 1985.
- De La Pierre, M. and Belmonte, D.: Ab initio investigation of majorite and pyrope garnets: lattice dynamics and vibrational spectra, *Am. Mineral.*, 101, 162–174, <https://doi.org/10.2138/am-2016-5382>, 2016.
- De La Pierre, M., Orlando, R., Maschio, L., Doll, K., Ugliengo, P., and Dovesi, R.: Performance of six functionals (LDA, PBE, PBESOL, B3LYP, PBE0, and WC1LYP) in the simulation of vibrational and dielectric properties of crystalline compounds. The case of forsterite  $\text{Mg}_2\text{SiO}_4$ , *J. Comput. Chem.*, 32, 1775–1784, <https://doi.org/10.1002/jcc.21750>, 2011.
- Demichelis, R., Civalleri, B., Ferrabone, M., and Dovesi, R.: On the performance of eleven DFT functionals in the description of the vibrational properties of aluminosilicates, *Int. J. Quantum Chem.*, 110, 406–415, <https://doi.org/10.1002/qua.22301>, 2010.
- Deuss, A. and Woodhouse, J.: Seismic observations of splitting of the mid-transition zone discontinuity in Earth's mantle, *Science*, 294, 354–357, <https://doi.org/10.1126/science.1063524>, 2001.
- Deuss, A., Redfern, S. A. T., Chambers, K., and Woodhouse, J. H.: The nature of the 660-kilometer discontinuity in Earth's mantle from global seismic observations of PP precursors, *Science*, 311, 198–201, <https://doi.org/10.1126/science.1120020>, 2006.
- Dorogokupets, P. I., Dymshits, A. M., Sokolova, T. S., Danilov, B. S., and Litasov, K. D.: The equations of state of forsterite, wadsleyite, ringwoodite, akimotoite,  $\text{MgSiO}_3$ -perovskite, and post-perovskite and phase diagram for the  $\text{Mg}_2\text{SiO}_4$  system at pressures of up to 130 GPa, *Russ. Geol. Geophys.*, 56, 172–189, <https://doi.org/10.1016/j.rgg.2015.01.011>, 2015.
- Dovesi, R., Saunders, V. R., Roetti, C., Orlando, R., Zicovich-Wilson, C. M., Pascale, F., Civalleri, B., Doll, K., Harrison, N. M., and Bush, I. J.: CRYSTAL14 User's Manual, Università di Torino, Torino, Italy, 382 pp., <https://www.crystal.unito.it/Manuals/crystal14.pdf> (last access: 23 March 2022), 2014.
- Dziewonski, A. M. and Anderson, D. L.: Preliminary reference Earth model, *Phys. Earth Planet. Int.*, 25, 297–356, [https://doi.org/10.1016/0031-9201\(81\)90046-7](https://doi.org/10.1016/0031-9201(81)90046-7), 1981.
- Erba, A., Mahmoud, A., Belmonte, D., and Dovesi, R.: High pressure elastic properties of minerals from ab initio simulations: the case of pyrope, grossular and andradite silicate garnets, *J. Chem. Phys.*, 140, 124703, <https://doi.org/10.1063/1.4869144>, 2014.
- Evarestov, R. A. and Losev, M. V.: All-electron LCAO calculations of the LiF crystal phonon spectrum: influence of the basis set, the exchange-correlation functional, and the supercell size, *J. Comput. Chem.*, 30, 2645–2655, <https://doi.org/10.1002/jcc.21259>, 2009.
- Fabrichnaya O. B., Saxena, S. K., Richet, P., and Westrum, E. F.: Thermodynamic Data, Models, and Phase Diagrams in Multicomponent Oxide Systems, Springer, Berlin Heidelberg, Germany, 198 pp., <https://doi.org/10.1007/978-3-662-10504-7>, 2004.
- Feng, L., Lin, Y., Hu, S., Xu, L., and Miao, B.: Estimating compositions of natural ringwoodite in the heavily shocked Grove Mountains 052049 meteorite from Raman spectra, *Am. Mineral.*, 96, 1480–1489, <https://doi.org/10.2138/am.2011.3679>, 2011.
- Fiquet, G., Richet, P., and Montagnac, G.: High-temperature thermal expansion of lime, periclase, corundum and spinel, *Phys. Chem. Minerals*, 27, 103–111, <https://doi.org/10.1007/s002690050246>, 1999.
- Frost, D. J.: The structure and sharpness of  $(\text{Mg,Fe})_2\text{SiO}_4$  phase transformations in the transition zone, *Earth Planet. Sci. Lett.*, 216, 313–328, [https://doi.org/10.1016/S0012-821X\(03\)00533-8](https://doi.org/10.1016/S0012-821X(03)00533-8), 2003.
- Guyot, F., Boyer, H., Madon, M., Velde, B., and Poirier, J. P.: Comparison of the Raman microprobe spectra of  $(\text{Mg,Fe})_2\text{SiO}_4$  and  $\text{Mg}_2\text{GeO}_4$  with olivine and spinel structures, *Phys. Chem. Miner.*, 13, 91–95, <https://doi.org/10.1007/BF00311898>, 1986.
- Hazen, R. M.: Comparative compressibilities of silicate spinels: anomalous behaviour of  $(\text{Mg,Fe})_2\text{SiO}_4$ , *Science*, 259, 206–209, <https://doi.org/10.1126/science.259.5092.206>, 1993.
- Helffrich, G.: Practical use of Suzuki's thermal expansivity formulation, *Phys. Earth Planet. Int.*, 116, 133–136, [https://doi.org/10.1016/S0031-9201\(99\)00130-2](https://doi.org/10.1016/S0031-9201(99)00130-2), 1999.
- Hernández, E. M., Brodholt, J., and Alfè, D.: Structural, vibrational and thermodynamic properties of  $\text{Mg}_2\text{SiO}_4$  and  $\text{MgSiO}_3$  minerals from first-principles simulations, *Phys. Earth Planet. Int.*, 240, 1–24, <https://doi.org/10.1016/j.pepi.2014.10.007>, 2015.
- Holland, T. J. B. and Powell, R.: An improved and extended internally consistent thermodynamic dataset for phases of petrological interest, involving a new equation of state for solids, *J. Metam. Geol.*, 29, 333–383, <https://doi.org/10.1111/j.1525-1314.2010.00923.x>, 2011.
- Inoue, T., Tanimoto, Y., Irifune, T., Suzuki, T., Fukui, H., and Ohtaka, O.: Thermal expansion of wadsleyite, ringwoodite, hydrous wadsleyite and hydrous ringwoodite, *Phys. Earth Planet. Int.*, 143–144, 279–290, <https://doi.org/10.1016/j.pepi.2003.07.021>, 2004.
- Ishii, T., Huang, R., Myhill, R., Fei, H., Koemets, I., Liu, Z., Maeda, F., Yuan, L., Wang, L., Druzhbin, D., Yamamoto, T., Bhat, S., Farla, R., Kawazoe, T., Tsujino, N., Kulik, E., Higo, Y., Tange, Y., and Katsura, T.: Sharp 660 km discontinuity controlled by extremely narrow binary post-spinel transition, *Nat. Geosci.*, 12, 869–872, <https://doi.org/10.1038/s41561-019-0452-1>, 2019.
- Jacobs, M. H. G., Schmid-Fetzer, R., and van den Berg, A. P.: Phase diagrams, thermodynamic properties and sound velocities derived from a multiple Einstein method using vibrational densities of states: an application to  $\text{MgO-SiO}_2$ , *Phys. Chem. Miner.*, 44, 43–62, <https://doi.org/10.1007/s00269-016-0835-4>, 2017.
- Jeanloz, R.: Infrared spectra of olivine polymorphs:  $\alpha$ ,  $\beta$  phase and spinel, *Phys. Chem. Minerals*, 5, 327–341, <https://doi.org/10.1007/BF00307542>, 1980.
- Katsura, T., Yokoshi, S., Song, M., Kawabe, K., Tsujimura, T., Kubo, A., Ito, E., Tange, Y., Tomioka, N., Saito, K., Nozawa, A., and Funakoshi, K.-I.: Thermal expansion of  $\text{Mg}_2\text{SiO}_4$  ringwoodite at high pressures, *J. Geophys. Res.-Sol. Ea.*, 109, B12209, <https://doi.org/10.1029/2004JB003094>, 2004.
- Katsura, T., Yoneda, A., Yamazaki, D., Yoshino, T., and Ito, E.: Adiabatic temperature profile in the mantle, *Phys. Earth Planet. Int.*, 183, 212–218, <https://doi.org/10.1016/j.pepi.2010.07.001>, 2010.
- Kiefer, B., Stixrude, L., and Wentzcovitch, R. M.: Calculated elastic constants and anisotropy of  $\text{Mg}_2\text{SiO}_4$  spinel

- at high pressure, *Geophys. Res. Lett.*, 24, 2841–2844, <https://doi.org/10.1029/97GL02975>, 1997.
- Kiefer, B., Stixrude, L., and Wentzcovitch, R.: Normal and inverse ringwoodite at high pressures, *Am. Mineral.*, 84, 288–293, <https://doi.org/10.2138/am-1999-0311>, 1999.
- Kohanoff, J.: *Electronic Structure Calculations for Solids and Molecules: Theory and Computational Methods*, Cambridge University Press, Cambridge, UK, ISBN 9780521815918, 2006.
- Kojitani, H., Inoue, T., and Akaogi, M.: Precise measurements of enthalpy of postspinel transition in  $\text{Mg}_2\text{SiO}_4$  and application to the phase boundary calculation, *J. Geophys. Res.-Sol. Ea.*, 121, 729–742, <https://doi.org/10.1002/2015JB012211>, 2016.
- Lee, C., Yang, E., and Parr, R. G.: Development of the Colle-Salvetti correlation-energy formula into a functional of the electron density, *Phys. Rev. B*, 37, 785–789, <https://doi.org/10.1103/PhysRevB.37.785>, 1988.
- Li, L., Weidner, D. J., Brodholt, J., Alfè, D., and Price, G. D.: Elasticity of  $\text{Mg}_2\text{SiO}_4$  ringwoodite at mantle conditions, *Phys. Earth Planet. Int.*, 157, 181–187, <https://doi.org/10.1016/j.pepi.2006.04.002>, 2006.
- Li, L., Brodholt, J., and Alfè, D.: Structure and elasticity of hydrous ringwoodite: a first principle investigation, *Phys. Earth Planet. Int.*, 177, 103–115, <https://doi.org/10.1016/j.pepi.2009.07.007>, 2009.
- McMillan, P. and Akaogi, M.: Raman spectra of  $\beta\text{-Mg}_2\text{SiO}_4$  (modified spinel) and  $\gamma\text{-Mg}_2\text{SiO}_4$  (spinel), *Am. Mineral.*, 72, 361–364, 1987.
- Meng, Y., Weidner, D. J., Gwanmesia, G. D., Liebermann, R. C., Vaughan, M. T., Wang, Y., Leinenweber, K., Pacalo, R. E., Yeganeh-Haeri, A., and Zhao, Y.: In situ high  $P$ - $T$  X ray diffraction studies on three polymorphs ( $\alpha$ ,  $\beta$ ,  $\gamma$ ) of  $\text{Mg}_2\text{SiO}_4$ , *J. Geophys. Res.-Sol. Ea.*, 98, 22199–22207, <https://doi.org/10.1029/93JB02383>, 1993.
- Meng, Y., Fei, Y., Weidner, D. J., Gwanmesia, G. D., and Hu, J.: Hydrostatic compression of  $\gamma\text{-Mg}_2\text{SiO}_4$  to mantle pressures and 700 K: thermal equation of state and related thermoelastic properties, *Phys. Chem. Minerals*, 21, 407–412, <https://doi.org/10.1007/BF00203299>, 1994.
- Ming, L. C., Manghnani, M. H., Kim, Y. H., Usha-Devi, S., Xu, J.-A., and Ito, E.: Thermal expansion studies of  $(\text{Mg,Fe})_2\text{SiO}_4$ -spinel using synchrotron radiation, in: *Thermodynamic Data: Systematics and Estimation*, Advances in Physical Geochemistry, Vol. 10, edited by: Saxena, S. K., Springer-Verlag, New York, NY, 315–334, [https://doi.org/10.1007/978-1-4612-2842-4\\_12](https://doi.org/10.1007/978-1-4612-2842-4_12), 1992.
- Nestola, F.: Ringwoodite: its importance in Earth Sciences, in: *Highlights in Mineralogical Crystallography*, edited by: Armbruster, T. and Danisi, R. M., De Gruyter, Berlin, Germany, 127–147, <https://doi.org/10.1515/9783110417104-007>, 2016.
- Núñez-Valdez, M., da Silveira, P., and Wentzcovitch, R. M.: Influence of iron on the elastic properties of wadsleyite and ringwoodite, *J. Geophys. Res.-Sol. Ea.*, 116, B12207, <https://doi.org/10.1029/2011JB008378>, 2011.
- Oganov, A. R., Brodholt, J. P., and Price, G. D.: Ab initio elasticity and thermal equation of state of  $\text{MgSiO}_3$  perovskite, *Earth Planet. Sci. Lett.*, 184, 555–560, [https://doi.org/10.1016/S0012-821X\(00\)00363-0](https://doi.org/10.1016/S0012-821X(00)00363-0), 2001.
- Otonello, G., Civalleri, B., Ganguly, J., Vetuschi Zuccolini, M., and Noel, Y.: Thermophysical properties of the  $\alpha$ - $\beta$ - $\gamma$  polymorphs of  $\text{Mg}_2\text{SiO}_4$ : a computational study, *Phys. Chem. Minerals*, 36, 87–106, <https://doi.org/10.1007/s00269-008-0260-4>, 2009.
- Otonello, G., Civalleri, B., Ganguly, J., Perger, W. F., Belmonte, D., and Vetuschi Zuccolini, M.: Thermo-chemical and thermo-physical properties of the high-pressure phase anhydrous B ( $\text{Mg}_{14}\text{Si}_5\text{O}_{24}$ ): an ab-initio all-electron investigation, *Am. Mineral.*, 95, 563–573, <https://doi.org/10.2138/am.2010.3368>, 2010.
- Panero, W. R.: Cation disorder in ringwoodite and its effects on wave speeds in the Earth’s transition zone, *J. Geophys. Res.-Sol. Ea.*, 113, B10204, <https://doi.org/10.1029/2008JB005676>, 2008.
- Parlinski, K., Li, Z. Q., and Kawazoe, Y.: First-principles determination of the soft mode in cubic  $\text{ZrO}_2$ , *Phys. Rev. Lett.*, 78, 4063–4066, <https://doi.org/10.1103/PhysRevLett.78.4063>, 1997.
- Pearson, D. G., Brenker, F. E., Nestola, F., McNeill, J., Nasdala, L., Hutchison, M. T., Matveev, S., Mather, K., Silversmit, G., Schmitz, S., Vekemans, B., and Vincze, L.: Hydrous mantle transition zone indicated by ringwoodite included within diamond, *Nature*, 507, 221–224, <https://doi.org/10.1038/nature13080>, 2014.
- Piekarz, P., Jochym, P. T., Parlinski, K., and Łazewski, J.: High-pressure and thermal properties of  $\gamma\text{-Mg}_2\text{SiO}_4$  from first-principles calculations, *J. Chem. Phys.*, 117, 3340–3344, <https://doi.org/10.1063/1.1494802>, 2002.
- Prencipe, M., Noel, Y., Bruno, M., and Dovesi, R.: The vibrational spectrum of lizardite-1T [ $\text{Mg}_3\text{Si}_2\text{O}_5(\text{OH})_4$ ] at the  $\Gamma$  point: a contribution from an ab initio periodic B3LYP calculation, *Am. Mineral.*, 94, 986–994, <https://doi.org/10.2138/am.2009.3127>, 2009.
- Prencipe, M., Bruno, M., Nestola, F., De La Pierre, M., and Nimis, P.: Toward an accurate ab initio estimation of compressibility and thermal expansion of diamond in the [0, 3000 K] temperature and [0, 30 GPa] pressures ranges, at the hybrid HF/DFT theoretical level, *Am. Mineral.*, 99, 1147–1154, <https://doi.org/10.2138/am.2014.4772>, 2014.
- Preudhomme, J. and Tarte, P.: Infrared studies of spinels – II. The experimental bases for solving the assignment problem, *Spectrochim. Acta*, 27A, 845–851, [https://doi.org/10.1016/0584-8539\(71\)80163-0](https://doi.org/10.1016/0584-8539(71)80163-0), 1971.
- Ringwood, A. E.: *Composition and Petrology of the Earth’s Mantle*, McGraw-Hill, New York, NY, <https://doi.org/10.1180/minmag.1977.041.317.30>, 1975.
- Saikia, A., Frost, D. J., and Rubie, D. C.: Splitting of the 520-kilometer seismic discontinuity and chemical heterogeneity in the mantle, *Science*, 319, 1515–1518, <https://doi.org/10.1126/science.1152818>, 2008.
- Sasaki, S., Prewitt, C. T., Sato, Y., and Ito, E.: Single-crystal X ray study of  $\gamma\text{-Mg}_2\text{SiO}_4$ , *J. Geophys. Res.-Sol. Ea.*, 87, 7829–7832, <https://doi.org/10.1029/JB087iB09p07829>, 1982.
- Schmeling, H., Marquart, G., and Ruedas, T.: Pressure- and temperature-dependent thermal expansivity and the effect on mantle convection and surface observables, *Geophys. J. Int.*, 154, 224–229, <https://doi.org/10.1046/j.1365-246X.2003.01949.x>, 2003.
- Schmerr, N. and Garnero, E. J.: Upper mantle discontinuity topography from thermal and chemical heterogeneity, *Science*, 318, 623–626, <https://doi.org/10.1126/science.1145962>, 2007.
- Shearer, P. M.: Transition zone velocity gradients and the 520 km discontinuity, *J. Geophys. Res.-Sol. Ea.*, 101, 3053–3066, <https://doi.org/10.1029/95JB02812>, 1996.

- Sinogeikin, S. V., Bass, J. D., and Katsura, T.: Single-crystal elasticity of ringwoodite to high pressures and high temperatures: implications for 520 km seismic discontinuity, *Phys. Earth Planet. Int.*, 136, 41–66, [https://doi.org/10.1016/S0031-9201\(03\)00022-0](https://doi.org/10.1016/S0031-9201(03)00022-0), 2003.
- Stixrude, L. and Lithgow-Bertelloni, C.: Thermodynamics of mantle minerals – I. Physical properties, *Geophys. J. Int.*, 162, 610–632, <https://doi.org/10.1111/j.1365-246X.2005.02642.x>, 2005.
- Suzuki, I., Ohtani, E., and Kumazawa, M.: Thermal expansion of  $\gamma$ -Mg<sub>2</sub>SiO<sub>4</sub>, *J. Phys. Earth*, 27, 53–61, <https://doi.org/10.4294/jpe1952.27.53>, 1979.
- Thiéblot, L., Roux, J., and Richet, P.: High-temperature thermal expansion and decomposition of garnets, *Eur. J. Mineral.*, 10, 7–15, <https://doi.org/10.1127/ejm/10/1/0007>, 1998.
- Tosi, N., Yuen, D. A., de Koker, N., and Wentzcovitch, R. M.: Mantle dynamics with pressure- and temperature-dependent thermal expansivity and conductivity, *Phys. Earth Planet. Int.*, 217, 48–58, <https://doi.org/10.1016/j.pepi.2013.02.004>, 2013.
- Ulian, G. and Valdrè, G.: Equation of state of hexagonal hydroxylapatite (P6<sub>3</sub>) as obtained from density functional theory simulations, *Int. J. Quantum Chem.*, 118, e25553, <https://doi.org/10.1002/qua.25553>, 2018.
- Wallace, D. C.: *Thermodynamics of Crystals*, John Wiley & Sons, Inc., New York, NY, ISBN 9780471918554, 1972.
- White, W. B. and DeAngelis, B. A.: Interpretation of the vibrational spectra of spinels, *Spectrochim. Acta*, 23A, 985–993, [https://doi.org/10.1016/0584-8539\(67\)80023-0](https://doi.org/10.1016/0584-8539(67)80023-0), 1967.
- Yu, Y. G. and Wentzcovitch, R. M.: Density functional study of vibrational and thermodynamic properties of ringwoodite, *J. Geophys. Res.-Sol. Ea.*, 111, B12202, <https://doi.org/10.1029/2006JB004282>, 2006.